Simulation of kinematic and dynamic models of frontal shearer for coal mining automation process

Authors:
Toleukhan Ermekov, Muratbek Arpabekov, Zhaken Kuanyshbaev
L.N.Gumilyov Eurasian National University
010000, Astana/Republik Kasachstan

Summary: Coal mining industry is important economic field for prosperity and development of country economics, however providing safety, productivity and environmental sustainability of underground coal mining process is highly complex issue. It can be achieved through complex automation. In order to design control system hardware a mathematical model of frontal shearer has to be examined. The kinematic and dynamic models of frontal shearer (FEM-5) has been evaluated and then the systems with different initial parameters has been tested for stability according to Hurwitz criteria. The system has been examined for closed-loop and opened-loop stability with different values of proportional controller which has shown its stability in marginal position.

1 Introduction

For purpose of robotics and automation of the production processes, environmental security and measures to minimize the environment negative impact on people are the priority directions of the adopted by Government of the Republic of Kazakhstan concept of the Kazakhstan's mining industry development for the period till 2020 [1].

At that the existing technologies require continuous presence of people in stope with unfavorable and hazardous for health environment (high content of dust and gas, injury risks) that has serious social consequences. In addition to these miners may stay in zone of gas and coal dust explosion or get poisoned with toxic gases such as CH_4 and CO which requires to implement more expensive, time consuming rescue operation [2]. Hence, there exists the big economic problem of improvement, such as coal extraction effectiveness, increase of the extracted products quality, avoidance from the hard hand labor execution by people in areas with unfavorable conditions. Waste-free technology of coal-bearing layers' extraction implementation on the basis of mining robotics is the most effective way of this objective achievement.

For automation process of extraction of coal, the kinematic models and dynamics of FEM-5 (Mining Automated Extraction Manipulator) has to be evaluated prior making computer based programming. Dynamic control goal consists in receiving the required dynamic response from the RTC complex controlled by personal computer so that this response corresponds to some preliminarily determined multitude of criteria. These criteria may be expressed via impulse and forces of reaction and inertia impacting on the cutter crowns. Generally, the control problem consists in obtaining the main equations of the robot dynamics in the form of FEM-5 dynamic model and in further determination of control rules which will allow achieving the desired dynamic response.

As it was noted above, mining extraction manipulator controlled from computer may be modeled as open kinematic and dynamic circuit of several solid bodies (segments) subsequently connected by rotating joints. As we already know the solution of inverse kinematic problem [3], we find a set of integrated angles θ_1, which will allow giving to the cutter crown position and orientation set via T_i^0 in relation to the basic system of coordinates. In statics and dynamics of the robots we deal with integrated forces f_i and moments t_i, which allow achieving the required force f and moment t on the cutter crown. In such a way we deal with the inverse objective of the manipulators dynamics, that is, the task of calculating integrated moments required to obtain the preset generalized coordinates of speeds and accelerations.

There exist three approaches which allow obtaining the sum total of interlinked sufficiently non-linear differential equations describing the FEM-5 (Fig. 1) dynamics:

- dynamics presentation by the method of connected graphs (developed by Hank Painter in 1950);
- dynamics presentation by the Newton-Eiler method;
- dynamics presentation by the Lagrange-Eiler method.

In addition to these methods of presenting the dynamics of manipulation robots two recursive approaches are known. These are: Newton-Eiler recursive method and Lagrange recursive method. These recursive approaches allow sufficient reducing of the calculations number. Effectiveness of these methods is based on the sum total of recurrent links between the speeds, accelerations and integrated forces. Number of additions and multiplications in these methods changes in proportion to the number of joints (n) contrary to previous methods with dependences on the higher degrees' n [4].

1 General view of experimental manipulator FEM-5

The study has been started with longwall shearer automation research program of Longwall Automation Steering Committee (LASC) in Australia. This method is required to extract a seam in different level [5, 6].

2 Review in research of modeling kinematics of automated extraction manipulator

Operation of the narrow-grasp extraction manipulators is characterized by high dynamic loading. Analysis of the main factors determining the dynamic processes in manipulator made it possible to state that from among the number of all parameters of the manipulator the non-uniformity of delivery occurred as a result of small rigidness of traction member and a non-linear force of slipping friction is of the greatest importance.

Since the dynamics of the operating member drive load has a significant impact on the technological resource and productivity of the stopping robotic technology complex the reduction of load non-uniformity is and remains the primary and urgent objective. This objective is solved by different ways the most common of which are: increasing the delivery system rigidness, change of the breaking member design (layout of cutters) and increase of the advancing speed. According to the results of many researches the increase of delivery speed and rigidness of the advance systems are the most effective ways. At that [7, 8] the acceleration of the RTC delivery (at $V_n > 11$ m/min) leads to the loss of self-oscillation related to the friction factor. According to the research [9] the significant effect on change the rigidness factor of lowest natural frequencies has, and speed of delivery mostly impacts on highest natural frequencies.

For the mining automated extraction manipulator, the increase of delivery speed is limited by power resource; and increase of power supplied per job leads to the growth of weight and overall dimensions. Hence, the increase of the FEM-5 delivery rigidness is the most effective factor of reducing dynamic loads for FEM-5. Linking to this fact the research recommends rigidness of $C > 50 \cdot 10^5$ N/m for the extraction manipulator with mass = 6000 kg. In this case the self-oscillating nature of the delivery speed change is replaced by oscillation harmonic nature with the oscillation amplitude being less than the average value of speed.

It is necessary to note that L.P. Vozlublennaya, candidate of sciences in engineering, associate professor, in her research of the cone worm cutter crowns of winning machines of FEM-4, FEM-4KN, FEM-4N with consideration of structural and kinematic processes gives substantiation of three degrees of mobility which is the basis of solving the objective of above mentioned machines of FEM-5 type. The manipulator dynamics is determined by below listed values assigned as time functions t (Fig. 2): speed of extraction machine delivery along the face $v_n(t)$, angle of the face attack by manipulator $\alpha_0(t)$, angle velocity of the manipulator swing in horizontal plane $\omega_\alpha(t)$, angle speed of the manipulator boom swinging $\omega_c(t)$, angle of the manipulator boom turning $\varphi_c(t)$ in vertical plane [10].

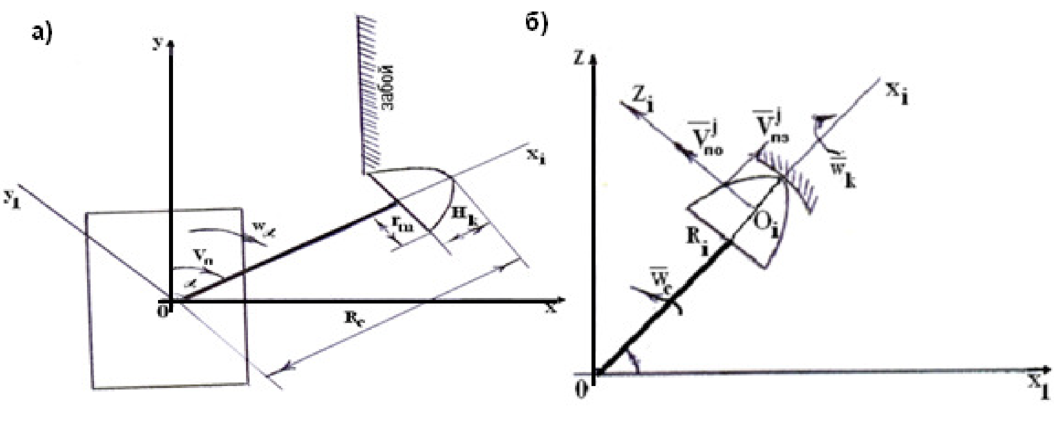

2 Kinematic model of advance of the manipulator with cutting operating member
a) in horizontal plane b) in vertical plane

Initial φ_{co}, α_{ko} and final φ_{ck}, α_{ck}, angles of the manipulator swinging in vertical and horizontal planes are assigned by ratios (at movement from the bottom up):

$$\varphi_{co} = -\arcsin\frac{H_M}{R_C}$$

$\varphi_{c} = \varphi_{c?}$

$$\varphi_{ck} = \arcsin\frac{H_{пл} - H_{м}}{R_C} \qquad (1)$$

$$\alpha_{ak} = \arcsin\frac{B_3 + \sin\alpha_0(R_c - H_k)}{R_C} - \frac{r_k c?s20}{R_C}$$

Angles $\varphi_c(t)$ and $\alpha_0(t)$ are determined as (3.2):

$$\varphi_c(t) = \varphi_{co} + \int_0^t \omega_c(t)dt$$

$$\alpha_0(t) = \alpha_{ak} + \int_0^t \omega_\alpha(t)dt \qquad (2)$$

where

- H_M = machine height in relation to ground by the manipulator rotation axis, m;
- R_C = length of the manipulator boom, m;
- H_K = length of the crown, m;
- H_K = extracting thickness of seam, m;
- $r_к$ = maximum radius of the crown, m.

Operating member (crown) of the manipulator rotates around its axis with frequency $n_{об}$ and has the length H_r and maximum radius (by base) $r_к$. For description of the manipulator movement let us match the basic system of coordinates 0_{xyz} with face and enter for description of each i-cutter located on the operating member the system of coordinates $0_i x_i y_i z_i$ rigidly tied with the plane of the i-cutter rotating together with the operating member. Mean value of the feed thrust is maintained automatically according to the consumed power on the operating member motor change of which leads to the change of consumption of the feed into hydraulic cylinders by the controlled pump NP 120 [7].

Computer simulating the movement of the operating member i-cutter and advancing the FEM-5 mining automated extraction manipulator. For computer simulation of the manipulator dynamics it is required to determine the following values and to add them in the MatLab-program code. Tasks for simulation modeling in MatLab environment are solved.

To determine the cutters configuration on the operating member the following below values serve:
$\Delta_{\gamma i}$ = central rotation angle between the i- and (i-1)-cutters [rad.];
Δ_{xi} = distance between ends of i- and (i-1)-cutters along the axis x_i [m];
Δ_{zi} = distance between ends of i- and (i+1)-cutters along the axis z_i [m];
$\Delta_{\varphi i}$ = central rotation angle between i-cutters and previous one in the same line of cutting (if the cutting line has one cutter then $\Delta_{\varphi i} = 2\pi$) [rad.].

Knowing the angle replacement of the operating member cutters it is possible to determine the initial rotation angle for i-cutters:

$$\gamma_{oi} = \sum_{j=1}^{i} \Delta\gamma_j \qquad (3)$$

In such a way by means of the above entered values one can determine for each cutter of operating member at any moment of time its coordinates in the basic system of coordinates 0_{xyz}, as well as its special orientation and location in relation to the neighbor cutters. This multitude of mathematical variables is the sum total of input parameters for research and creation of cuing model and load of the manipulator's operating member.

As it is obtained for the manipulator movement description it is necessary to match rigidly the basic system of coordinates 0_{xyz} with the face and to enter, for description of movement of each i-cutter placed on the operating member, the system of coordinates $0_i x_i y_i z_i$ rigidly bound with the plane of i-cutter end rotation together with operating member. Link between these two systems of coordinates is executed by formulas (4) and (5) where axis x_i and γ_i are bound with the manipulator axis direction and are used as intermediate elements for the link of the coordinates' system 0_{xyz} и $0_i x_i y_i z_i$.

$$\begin{cases} x = x_1 sin\alpha_0 - y_1 cos\alpha_0, \\ y = x_1 cos\alpha_0 + y_1 sin\alpha_0 \end{cases} \begin{cases} x_1 = xsin\alpha_0 + ycos\alpha_0, \\ y_1 = -xcos\alpha_0 + ysin\alpha_0, \end{cases} \qquad (4)$$

$$\begin{cases} x = x_1 sin\alpha_0 - y_1 cos\alpha_0, \\ y = x_1 cos\alpha_0 + y_1 sin\alpha_0 \end{cases} \begin{cases} x_1 = xsin\alpha_0 + ycos\alpha_0, \\ y_1 = -xcos\alpha_0 + ysin\alpha_0, \end{cases}$$
$$\begin{cases} x_i = \left(x_1 - sin\alpha_0 \int_0^t v_n(t)dt + z_i sin\varphi_0\right) \\ y_i = y_1 - cos\alpha_0 \cdot \int_0^t v_n(t)dt, \\ z_i = -\left(x_1 - sin\alpha_0 \int_0^t v_n(t)dt\right) sin\alpha_0 + z_1 cos\varphi_0. \end{cases} \qquad (5)$$

In the system of coordinates $0_i x_i y_i z_i$ position of the i-cuter end is determined (Fig. 3) by angle of its turn $\gamma_i(t)$ equal to:

$$\gamma_i(t) = \gamma_{oi} + 2\Pi n_{o6} t \qquad (6)$$

where γ_{oi} is the initial angle of i-cuter rotation.

Angle β_{zi} is different from zero only for the cutters the axis of which is deflected from the plane of i-cutter end rotation (or plane of cutting), otherwise, for the rotating cutters by which operating members of the FEM-5 mining automated extraction manipulators are equipped the angle β_{zi} is determined from condition that the i-cutter axis is located on the plane normal in relation to the operating member surface (for the crown this surface is parabolic):

$$\beta_{1i} = arccos\frac{2r_i H_k}{\sqrt{r_k^4 + 4r_i^2 H_i^2}} \quad (7)$$

where r_i – radius of the i-cutter base rotation, H_i is the distance between the crown end and the i-cuter base along the axis x_i.

Values r_i and H_i for the castellated operating member are bound by the ratio (8):

$$r_i = r_к\sqrt{H_i}/H_{к.} \quad (8)$$

Knowing angles β_{1i}, β_{2i} and the i-cutter length l one can determine any geometric characteristics of the cutter, in particular, the radius of i-cutter end rotation P_i:

$$P_i = \sqrt{r_i^2 + l^2(1 - sin^2\beta_{1i} \cdot \; tg^2\, \beta_{2i}) + 2r_i l \cdot sin\beta_{2i}} \quad (9)$$

Radius R_i of the center of the coordinates $0_i x_i y_i z_i$ (A points of O) system rotation in vertical plane is equal to:

$$R_i = R_c - H_i + l \cdot \sin\beta_{1i} \cdot \; tg\, \beta_{2i} \quad (10)$$

For determining the cutters configuration on the operating member the following below values serve:
$\Delta_{\gamma i}$ = central rotation angle between i- and (i-1) - cutters [rad.];
Δ_{xi} = distance between the i- and (i-1)-cutters ends along the axis x_i, [m];
Δ_{zi} = distance between the i- and (i+1)-cutters ends along the axis z_i, [m];
$\Delta_{\varphi i}$ = central rotation angle between the i- cutters and previous one in the same line of cutting (if in the cutting line there is only one cutter then $\Delta_{\varphi i}$ = 2п) [rad.].

Values Δ_{xi} and Δ_{zi} are calculated by formulas (11) and (12):

$$\Delta x_i = H_i - H_{i-1} + l \cdot \left(sin\beta_i \, tg\beta_{2i} - sin\beta_{1(i-1)} tg\, \beta_{2(i-1)})\right) \qquad (11)$$

$$\Delta z_i = P_{i+1} - P_i \qquad (12)$$

Knowing the angle displacement of the operating member cutters one can determine for the i-cutters their initial angle of rotation:

$$\gamma_{oi} = \sum_{j=1}^{i} \Delta\gamma_j \qquad (13)$$

In such a way by means of the above entered values one can determine for each cutter of operating member at any moment of time its coordinates in the basic system of coordinates 0_{xyz}, as well as its special orientation and location in relation to the neighbor cutters. This multitude of mathematical variables is the sum total of input parameters for research and creation of cuing model and load of the manipulator's operating member.

3 Dynamics of the mining automated extraction manipulator FEM-5

As the converters of the operating part angle advances and position sensor serve the synchro units one of which is required for determining the actual position of the operating part and another – for setting. Error signal via phase-sensitive amplifier is fed to the tracking drives and between actual position set by it is amplified by tandem amplifier of energy. Tracking drives transform the electric signals and mechanic moves of hydraulic amplifier spool executing the oil feeding in hydraulic cylinders of the operating member delivery.

As a basis for the system operation the principle of the executive member program control with the use of profiled cam dogs and the load of the cutting drive motor regulating according to current by means of the delivery speed change [11].

Transfer function of the transformer synchro operating in the transformer mode looks like $W_1(\delta) = K_1$, where K_1 is a factor of proportionality. Transfer function of the phase-sensitive amplifier is equal to: $W_1(\delta) = K_2$, where K_2 is the gain value.

According to works [89, 92] dynamic features of electrical part of the electric hydraulic tracking spool of PUMK type are described by the transfer function:

$$W_3(\eth) = \frac{\acute{O}_1(\eth)}{U_1(\eth)} = \frac{K\acute{y}}{A_4\eth^4 + A_3\eth^3 + A_2\eth^2 + A_1\eth + 1}, \qquad (14)$$

where

- Y_1 = is the advance of spool needle;
- U_1 = voltage of the spool feeding;
- K_3 = transfer factor.

For the hydraulic part the tracking drives of transfer function has the view:

$$W_4(\eth)=\frac{Q(\eth)}{\acute{O}_1(\eth)}=\frac{K_{\tilde{a}}}{(A_5\eth+1)\cdot(A_6\eth+1)}, \quad (15)$$

where
- Q = oil consumption;
- K_r = transfer factor.

For hydraulic amplifier of the spool type with rigid lever-type coupling the transfer function [7] looks like:

$$W_5(\eth)=\frac{K_3}{C_5\eth^2+C_6\eth+1}$$

Where K_3 is a transfer factor of hydraulic amplifier.

For hydraulic executive mechanism with hydraulic power cylinder of two-directional operation and spool control the transfer function has a view of integrating segment [12]:

$$W_6(\eth)=\frac{K_i}{\eth}$$

where K_m = the transfer function of hydraulic cylinder.

Transfer function of the open subsystem of horizontal feeding may by presented as:

$$W(\eth)=\frac{\hat{E}_1\cdot\hat{E}_2\cdot\hat{E}_{\acute{y}}\cdot\hat{E}_3\cdot\hat{E}_i}{(A_4\eth^4+A_3\eth^3+A_2\eth^2+A_l\eth+1)\cdot(A_5\eth+1)\cdot(A_6\eth+1)\cdot(C_5\eth^2+C_6\eth+1)}. \quad (18)$$

It is very difficult to determine the factor of this transfer function theoretically but in the work [89] it is shown that transfer function

$$W(p)=\frac{K_3K_{\text{г}}K_{\text{м}}}{(A_4p^4+A_3p^3+A_2p^2+A_lp+1)\cdot(A_6p+1)\cdot(A_6p+1)\cdot(C_5p^2+C_6p+1)} \quad (19)$$

may be approximated by the function of below type

$$W_{\text{B}}(\eth)=\frac{K}{T^2\eth^2+2E_1T_1\eth+1}, \quad (20)$$

where

- T_1 = 0,004c constant time;
- E_1 = 0,05 attenuation factor;

$K = 0{,}35\ \frac{\pi/MUH}{\text{В}}$

This transfer function is built for the segment the input parameter of which the voltage of tracking spool is, and output parameter is the fluid consumption, i.e. the transfer function of open subsystem may be presented as:

$$W_{cn}(\partial) = \frac{K_{cn}}{\partial \cdot \left(T_1^2\,\partial^2 + 2E_1T_1\,\partial + 1\right)}. \quad (21)$$

Let us examine this subsystem, i.e. check it for stability and appraise the quality of system at the assigned value of the input value error. Quality of tracking system is determined by accuracy of the input value reproducing.

Let us determine the gain value knowing the error value and value of the input signal change rate. Let us consider the steady-state condition, i.e. the impact changes with constant speed:

$$\Delta\psi = \frac{V}{K};\ \ K = \frac{V}{\Delta\psi}. \quad (22)$$

Then:

$$K_{cn} = \frac{0{,}046}{0{,}005} = 9{,}2.$$

Let us check the system for stability at such gain value:

$$W_{\tilde{n}\ddot{\imath}}(\partial) = \frac{9{,}2}{\partial\left[0{,}041^2\,\partial^2 + 2\cdot 0{,}05\cdot 0{,}041\,\partial + 1\right]},$$

Check according to the Gurvitz criterion shows that such system is not stable. In order to make the system stable it is necessary to enter correcting segments.
To determine the kind of correcting segment and its parameters we use the method of the logarithmic characteristics. Let us determine log-magnitude plot for

$$W_{\tilde{n}\ddot{\imath}}(\partial) = \frac{K_{\tilde{n}\ddot{\imath}}}{\partial\cdot\left(\alpha\cdot\partial^2 + b\partial + 1\right)},$$

where α =0,041^2; B = 0,0041 which looks like

$$L(w) = 20\lg\frac{k_{cn}}{p} - 20\lg\left(ap^2 + bp + 1\right),$$

Necessity in reproducing input impacts with the set accuracy leads to the certain requirements which shall be imposed to the low-frequency part of the logarithmic amplitude characteristic of the open system. In order to reproduce the input impacts with error being not more than the set one log-magnitude plot of the designed system shall be lower than the control point with coordinates:

$$w_k = \frac{\varepsilon_{max}}{V_{max}}, L_к(w) = 20\lg\frac{\delta_{max}}{\Delta\psi_{max}},$$ (25)

Where

$V_{\max} = 0{,}046\, рад/с -$

= maximum rate of the input signal change;

$\Delta\psi_{\max} = 0{,}5\% -$

= maximum error of the input signal reproducing;

$\delta = \frac{V_{\max}^2}{\varepsilon_{\max}} -$

= amplitude of the equivalent mode of the harmonic impact;

$\varepsilon_{\max} -$

= maximum acceleration of the input signal.

To the mid-frequency of logarithmic characteristic, the asymptote with single inclination corresponds. It passes in the interval of amplitudes:

$$\frac{M}{M-1} \geq A\cdot(\omega) \geq \frac{M}{M+1}.$$ (26)

Logarithmic frequency characteristic of the integrating segment is determined as:

$$\varphi(\omega) = -arctg\,\omega T_1 - arctg\,\omega T_2 = -arctg\frac{\omega\cdot(T_1 - T_2)}{1+\omega^2 T_1\cdot T_2} = -arctg\frac{\omega}{1+2\omega^2}$$ (27)

In the field of high frequencies let us make the inclination LAC matching with the inclination of actual LAC as high-frequency plot does not effect on the quality and stability of the system. Then the characteristic of correcting segment will have the transfer function looking like:

$$W(\partial) = K\frac{1+T_2\,\partial}{1+T_1\,\partial}\cdot\frac{1+T_4\,\partial}{1+T_3\,\partial}.$$ (28)

where

$$T_1 = \frac{1}{w_1} = \frac{1}{0{,}49} = 2c., T_2 = \frac{1}{w_2} = \frac{1}{1{,}0} = 1c., T_3 = \frac{1}{w_3} = \frac{1}{5{,}2} = 0{,}19c., T_4 = \frac{1}{w_4} = \frac{1}{24{,}4} = 0{,}041c.$$

Then transfer function of the open corrected system will have a view of:

$$W_{ck}(\partial) = \frac{9{,}2K\cdot(1+\partial)\cdot(1+0{,}041\partial)}{\partial\cdot(0{,}041^2\,\partial^2 + 0{,}0041\partial + 1)\cdot(1+2\partial)\cdot(1+0{,}19\partial)}.$$

Apart from the stability requirements to the regulating system belong series of other requirements to which they shall comply depending on the operation conditions of the regulated object and which are used to be called as the quality indices. Let us appraise the quality of regulating process by indirect approximate method, that is, the method of distributing roots of the characteristic equation [11]. Oscillation of the system is conditioned by the oscillating segment.

To enhance the quality of regulating let us use the correction with the help of the inverse links. By trying parameters of transfer functions of the correcting segment and parameters of transfer functions of segments not covered by feedback one can achieve the set form of transition process.

Analysis of the various correcting segments effect on the regulation system quality showed that the combined correction posing the subsequently connected integrating segment satisfies the set requirements most completely and oscillating segment is covered by feedback by means of real differentiating segment. Transfer function of the closed system:

$$W_3(\partial) = \frac{W_p(\partial)}{1+W_p(\partial)} = \frac{\dfrac{W_1 K_2}{\partial(1+W_1W_2)}\hbar\dfrac{1+\mathrm{T}_1\partial}{1+\mathrm{T}_{11}\partial}}{1+\dfrac{W_1 K}{\partial(1+W_1W_2)}\hbar\dfrac{1+\mathrm{T}_1\partial}{1+\mathrm{T}_{11}\partial}K_1}, \quad (29)$$

where

$$W_1(\partial) = \frac{K}{\mathrm{T}_1^2\partial^2 + 2E_1\mathrm{T}_1\partial + 1}, \hbar W_2(\partial) = \frac{\partial\tau}{1+\partial\tau_3};$$
$$W_3\partial = \frac{W_1K_2(1+\mathrm{T}_2P)K_1}{(1+W_1W_2)\partial(1+\mathrm{T}_{11}\partial)+W_1K_2(1+\mathrm{T}_2\partial)K_1} \quad (30)$$

Structural diagram of subsystem for control in horizontal and vertical plane are shown in Fig. 3.

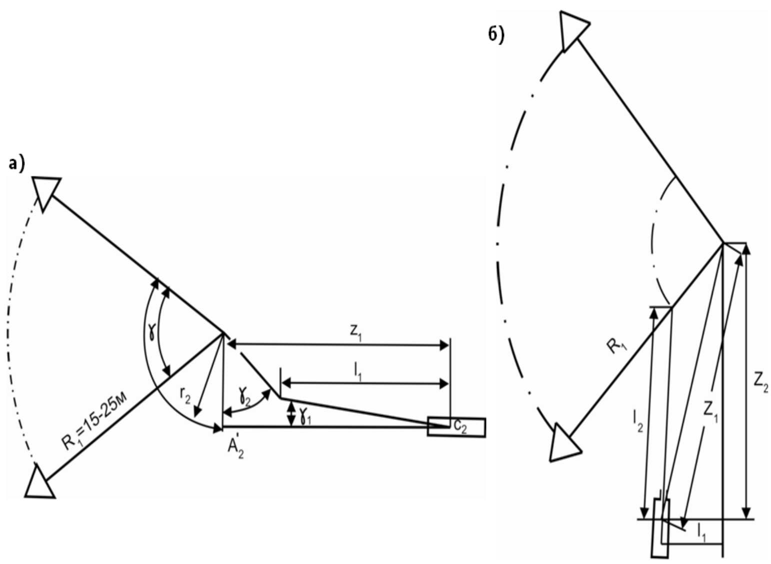

3 Schemes of the mechanisms for horizontal and vertical feeding
a) scheme of the horizontal feeding mechanism; b) scheme of the vertical feeding mechanism.

Transfer function of the closed-loop system looks like:

$$W_p(\partial) = \frac{K_{cn}}{\partial\left(T_1^2\partial^2 + 2E_1 T_1 \partial + 1\right)}. \quad (31)$$

Transfer function determines the error:

$$\Delta\varphi(\partial) = \frac{D(\partial)V}{PD(\partial) + K_{cn}^{/}}. \quad (32)$$

According to the Hurwitz criterion the system is unstable if the poles of systems re placed in the right half-plane. Let us examine this system for condition: whether it will provide the required error at this K_{cn}. For that we check whether the system characteristic does not come in the prohibited area of the log-magnitude plot system:

$$L(\omega) = 20\ell g\frac{K_{cn}^{/}}{p} - 20\ell g\left(\alpha \cdot p^2 + b_T \cdot p + 1\right). \quad (33)$$

Logarithmic characteristic of the first part of equation presents a straight line with slanting one and transiting through the point:

$$\omega = K_{cn}^{/} = 10{,}5.$$

Log-magnitude plot is determined by expression:

$$\varphi(\omega) = -\bar{\upsilon}\frac{\pi}{2} = -\frac{\pi}{2}. \quad (34)$$

Second component is similar to the expression earlier considered for the horizontal subsystem.

Building of the prohibited area of the mid-frequency plot:

$$20\ell g\frac{M}{M \cdot 1} \geq 20\ell g \cdot A \cdot (\omega) \geq 20\ell g\frac{M}{M+1},$$
$$12{,}73 \geq 20\ell g A \cdot (\omega) \geq 0{,}75. \quad (35)$$

From this expression it is seen that log-magnitude plot does not come into the prohibited area. Correcting segments for this subsystem are similar to those earlier accepted for the subsystem of horizontal feeding.

4 Results of Simulation

In Fig. 4 it is shown the motion trajectory of the manipulator's working part obtained by means of simulation modeling in MatLab at the preset parameters.

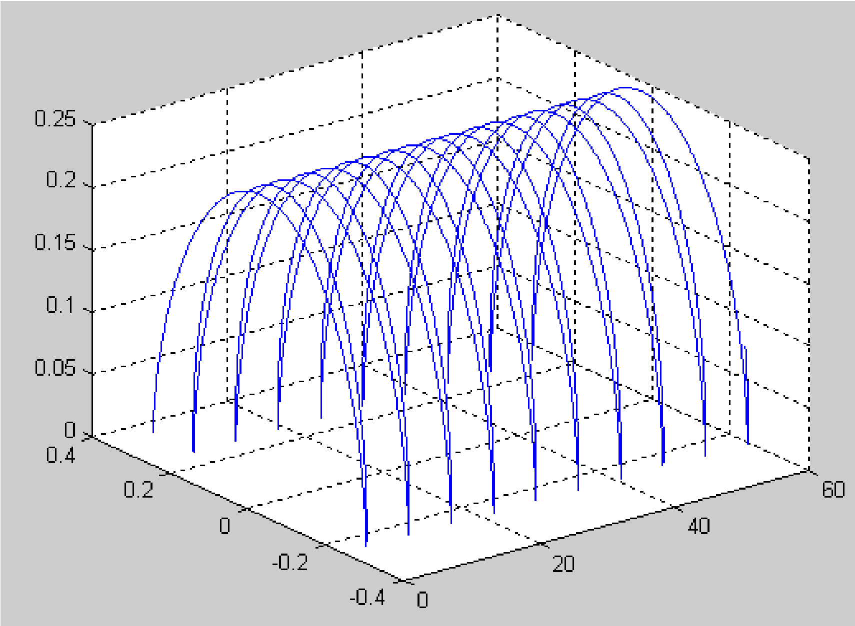

4 Simulation modeling of motion trajectory of the manipulator's working part

In Fig. 5 it is shown the trajectory of moving in the front plane of the manipulator's operating member i-cutter obtained by means of simulation modeling in MatLab at the preset parameters.

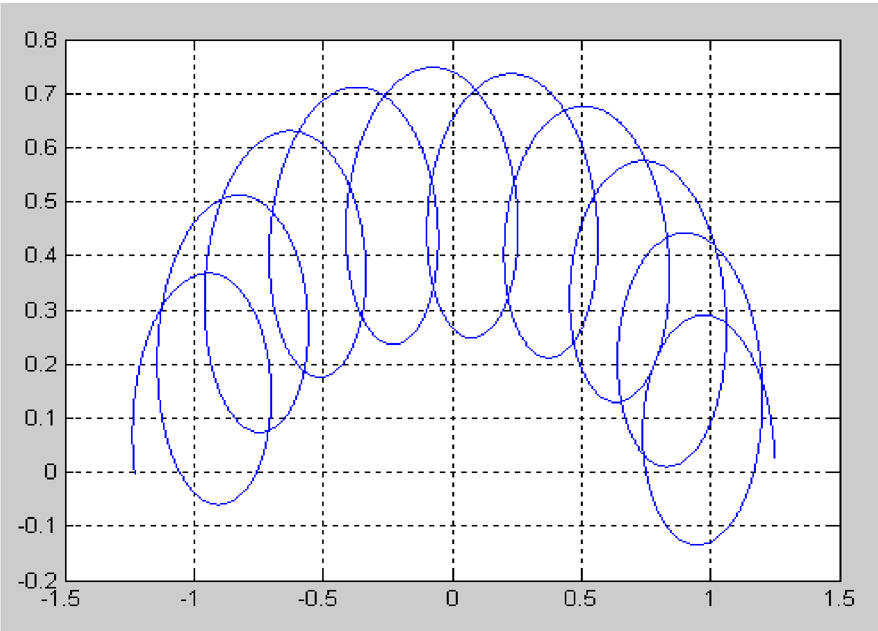

5 Modeling of the manipulator's operating part i-cutter motion in the front plane

In Fig. 6 it is shown the trajectory of the manipulator's operating member cutter moving in space obtained by means of simulation modeling in MatLab at the preset parameters.

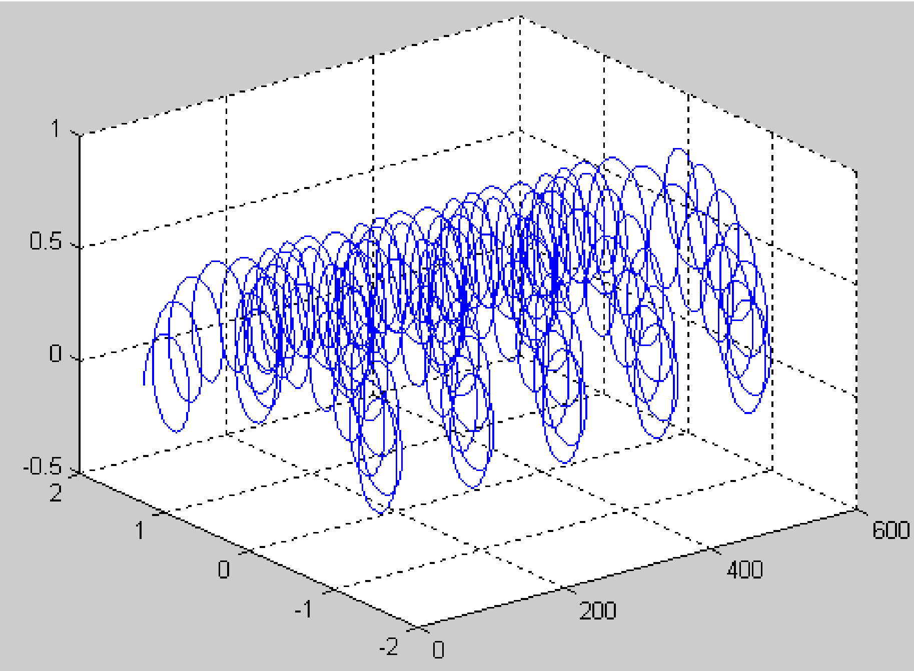

6 Simulation modeling of the manipulator's operating part i^{th} cutter motion in space

Using the functions of function mapping, for example, such as plot and plot 3, one can obtain trajectories and animations of the operating member movement. Fig. 7 presents an animation shot of the operating member moving at the set parameters.

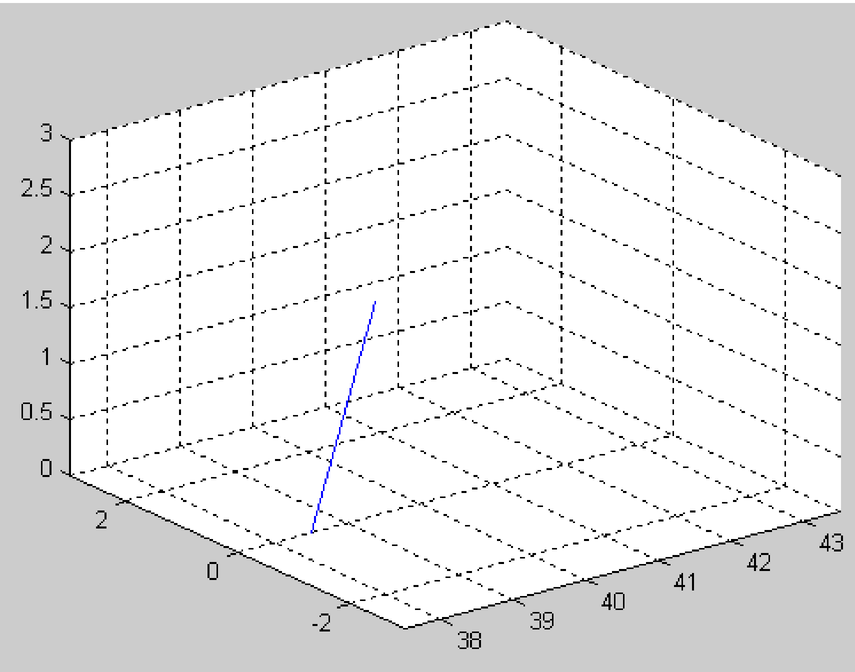

7 Screenshot of 3D motion of the cutting operating part of manipulator

In Fig. 8 it is shown the trajectory of the cutting operating part at the preset parameters of system, such as time interval and selected system of coordinates.

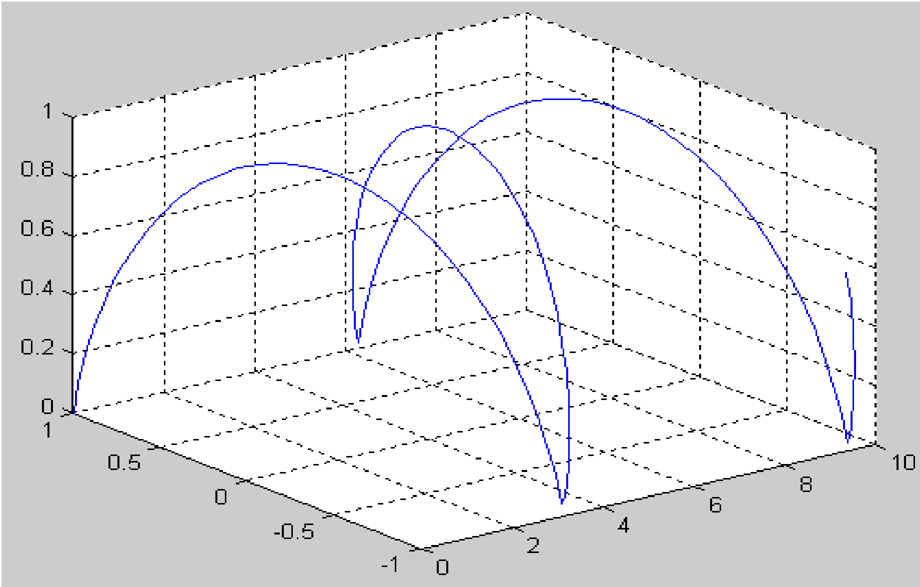

8 Motion trajectory of the operating part at the preset characteristics

5 Analysis of the dynamic characteristics of the FEM-5 manipulator control system as an automation items

The check for stability according to Hurwitz criterion showed the given system is stable at positive values of K but K<2. Let us examine the system behavior in vicinity to the stability limits for that we obtain characteristics at K = 0,1 and K = 2.

Case with K = 0,1.

In Fig. 9 a, the transient time of open-loop system is shown. Diagram of this transient time shows that the open-loop system is not stable.

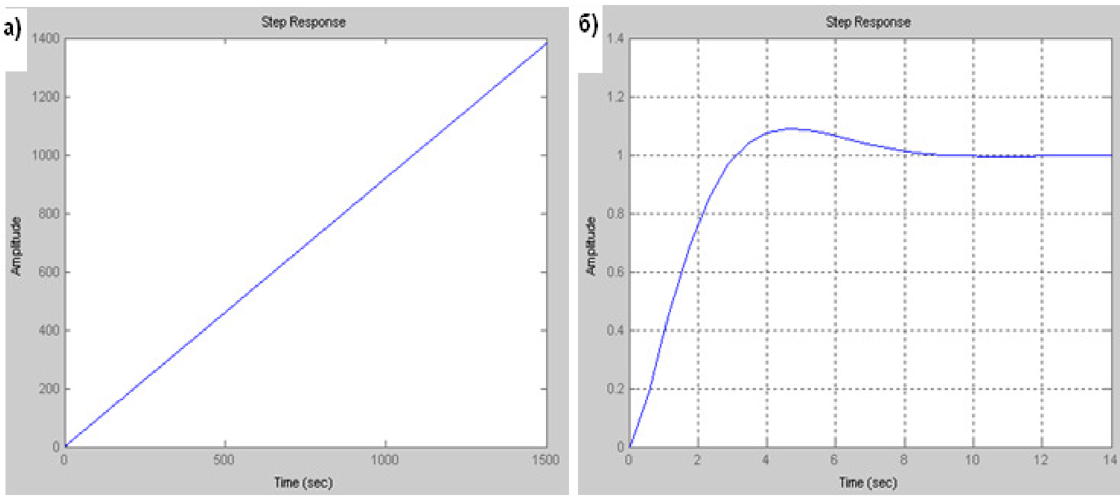

9 Checking for stability open-loop and closed-loop systems
a) transient time of the open-loop system; b) transient time of the closed-loop system

In Fig. 9 b transient time of the closed-loop system is shown. The diagram shows that the system in the course of time tends to the constant unit value and, hence, the closed system is stable. Let us make sure that the system is stable in relation to the values of the characteristic equation roots of the closed system. To obtain the layout let us use the command:

In Fig. 10 a, layout of the closed system roots is shown. All roots are posed in left half-plane of the complex plane; consequently, the closed-loop system is stable according to Lyapunov.

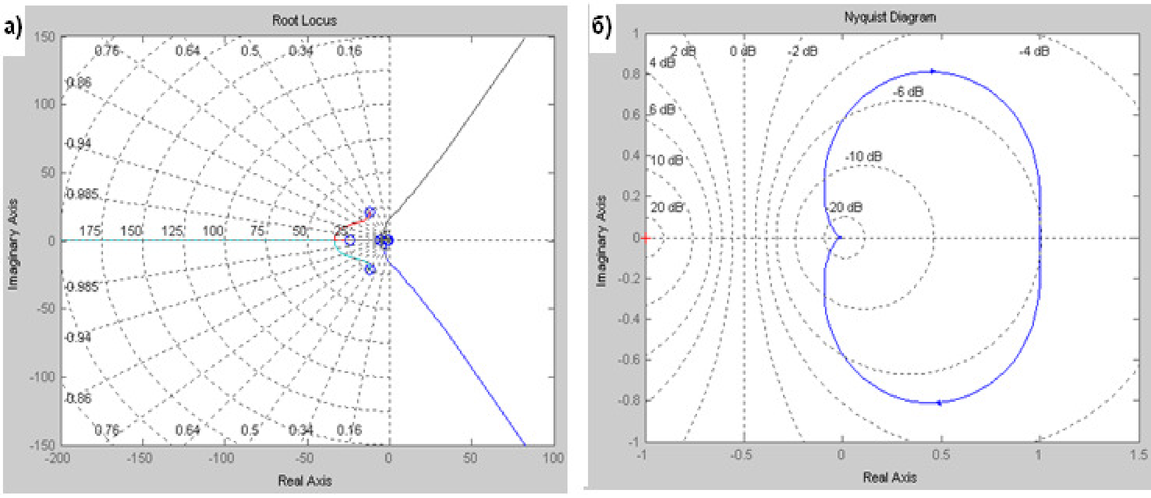

10 Check for stability of open-loop and closed-loop system by Root Locus and Nyquist Diagrams
a) closed-loop system's roots location; b) Nyquist Diagram of closed-loop system

In Fig. 10 b, Nyquist Diagram of the system is presented. Diagram starts on the positive real axis of the complex plane and by increase of the frequency it tends to the origin of plane, but not covering the point -1, j 0. Therefore, this system is stable according to the Nyquist criterion for closed-loop stability.

For completeness of the corrected system analysis we will obtain the Bode Plot characteristics.

Case with K = 2
Diagram in figure 11 a), also shows that the system at the value of parameter K=2 is stable as curve in the logarithmic scale crosses the level of 0 decibel earlier than the logarithmic phase-and-frequency characteristic crosses the level of 180°.

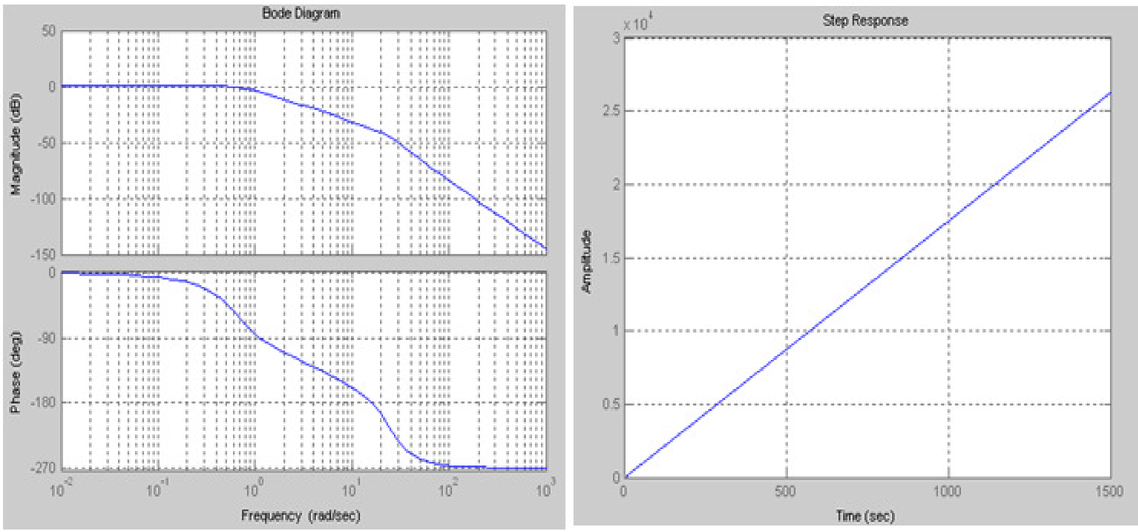

11 Check for stability according to the Hurwitz criterion
a) Logarithmic amplitude-and-phase-frequency characteristics; b) transition process of the closed system

In Fig. 11 b, transient time of the open-loop system is shown. Diagram of this transient time of step response shows that the system open-loop is not stable.

In Fig. 12 a, transient time of the closed-loop system is shown. Diagram shows that the system in the course of time tends to be the constant unit value and, hence, the closed-loop system is stable.

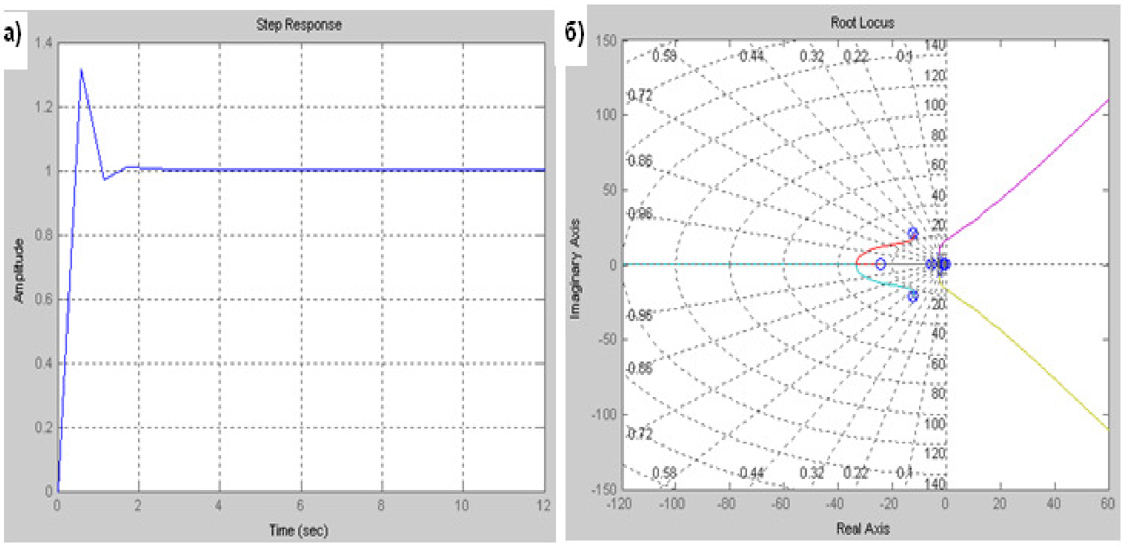

12 Check for stability according to the Hurwitz criterion
a) transition process of the closed-loop system; b) layout of the closed-loop system roots

In Fig. 13 a, the amplitude-and-phase characteristic of the closed control system is presented.

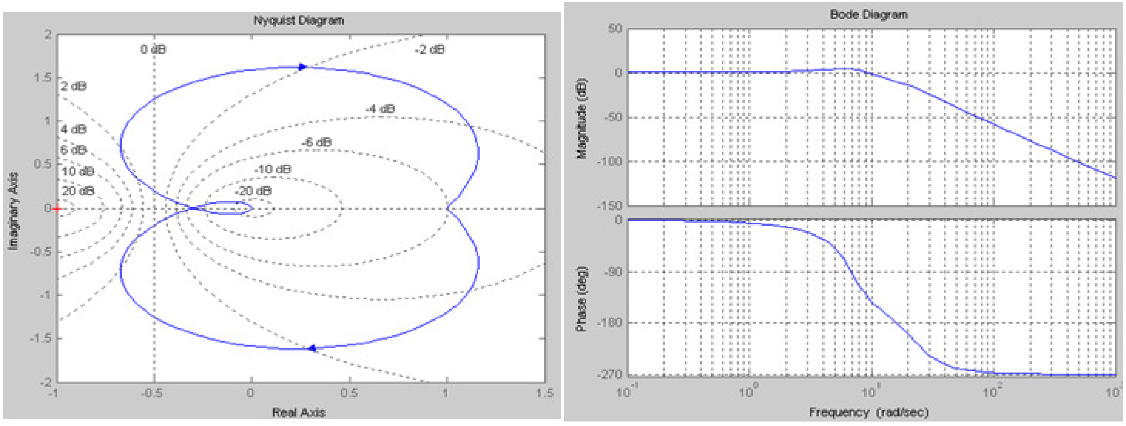

13 Check for stability according to the Hurwitz criterion
a) Nyquist diagram of the closed-loop control system; b) Bode plot diagrams of the logarithmic amplitude-and-phase-frequency characteristics

Amplitude-and-phase characteristic starts on the positive real axis of the complex plane and by increase of the frequency it tends to the beginning of coordinates not covering the point -1, j 0. Therefore, this system is stable according to the Nyquist criterion. In terms of analyses of stability of working part in vertical plane, it was found that this system is unstable.

In Fig. 14 a, transition process of the closed system is shown. Diagram of this transition process shows that the system is unstable.

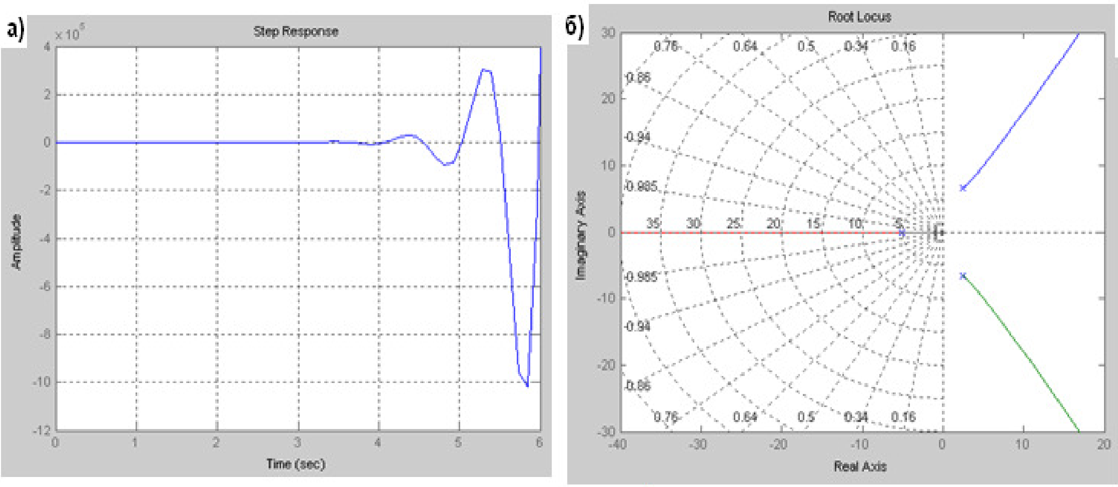

14 Check for stability according to the Hurvitz criterion
a) transition process of the closed system; b) layout of the closed system roots

In Fig. 14 b, layout of the closed-loop system roots is shown. Pair of complex conjugate roots is in the right half-plane of the complex plane, hence, the complex control system is unstable according to Lyapunov.

Let us examine the system behavior in the frequency field. In Fig. 15 a, the amplitude-and-phase characteristic of the control system is shown.

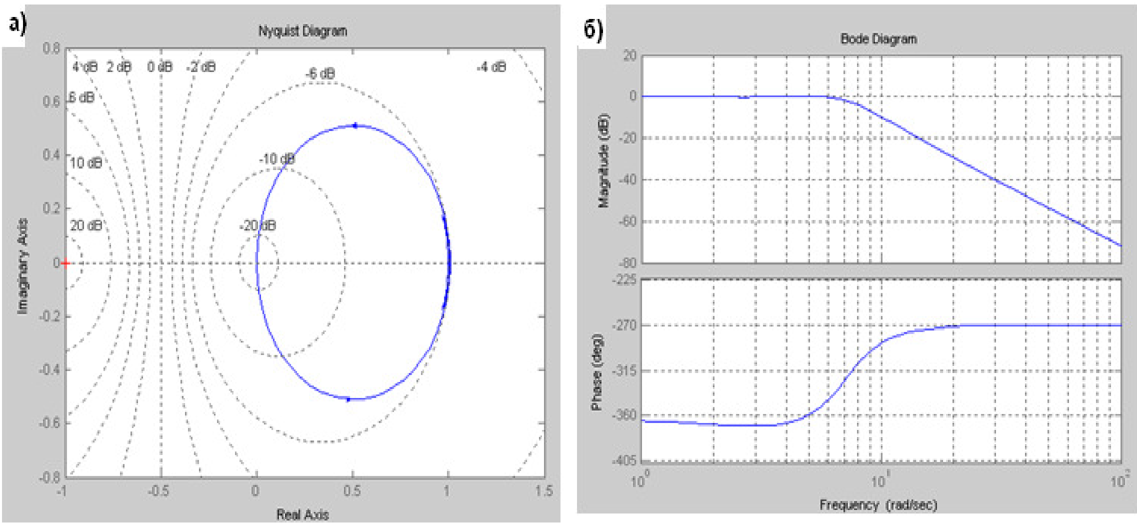

15 Amplitude-and-phase characteristic of the control system
a) amplitude-and-phase characteristic of the control system; b) logarithmic amplitude-and-phase-frequency characteristics

For completeness of the corrected system analysis we obtain logarithmic amplitude-and-phase-frequency characteristics. Diagrams of the logarithmic-and-phase-frequency characteristics are presented in fig. 15 b it also shows that system at the assigned values of parameters is unstable as the logarithmic amplitude-and-phase characteristic crosses the level of 0 decibel at the time when the phase-frequency characteristic has the level less than -180°. However, after this system examination for the condition whether it will provide the required error at this K_{cn} after check and whether it will not come into the prohibited area of the log-magnitude plot system it is seen that log-magnitude plot does not enter the prohibited area. Correcting segments for this subsystem are similar to those earlier accepted for the subsystem of horizontal feeding.

In Fig. 16 a), transition process of the closed system is shown.

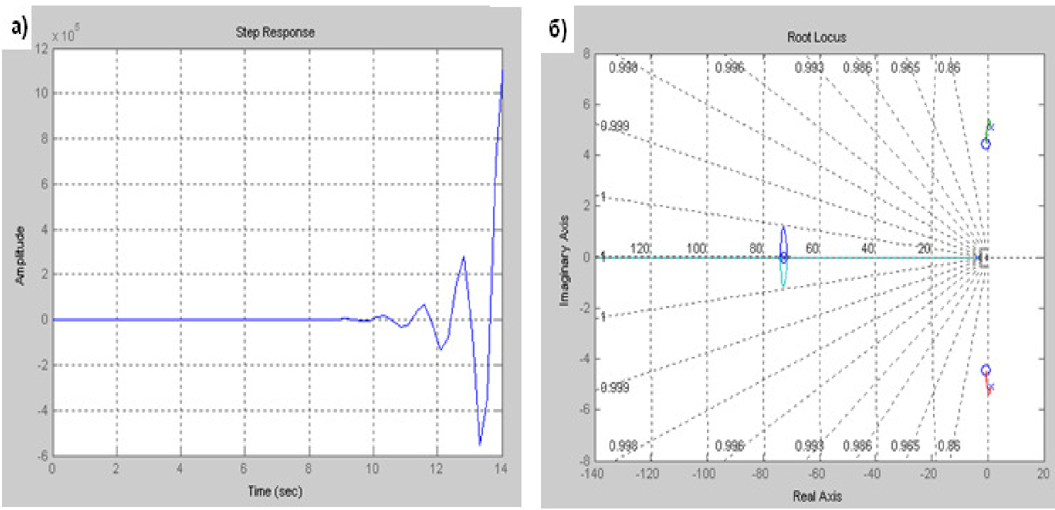

16 Transient process of the control system
a) transition process of the closed-loop system; b) Root-locus diagram of the closed-loop system

In Fig. 17 a, amplitude-and-phase characteristic with Nyquist diagram of the control system is presented.

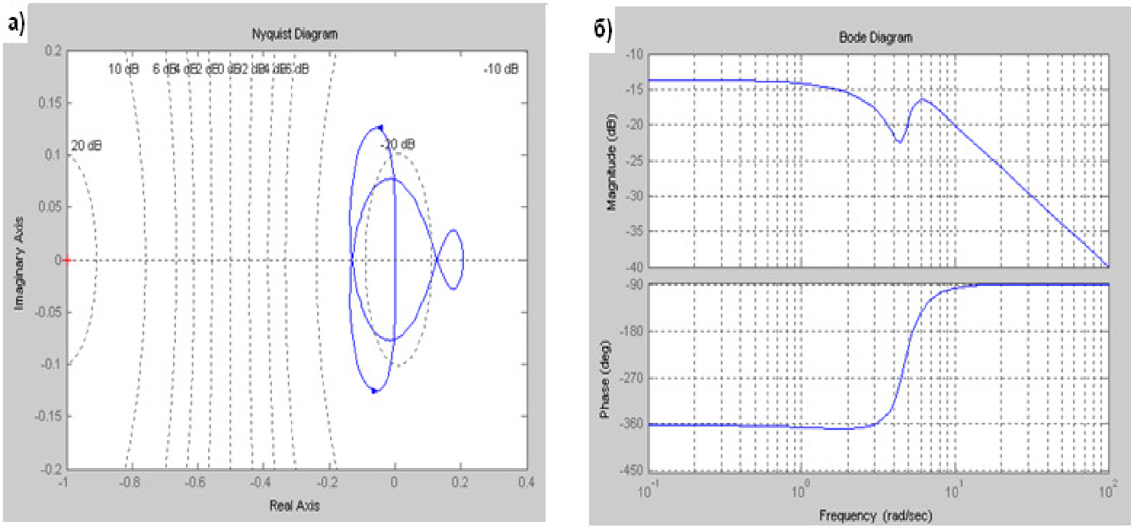

17 Characteristics of the control system
a) Nyquist diagram of the control system; b) Bode Plot diagram of the system

The characteristics of Bode Plot diagram are presented in Fig. 17 b.

6 Discussion

Kinematic analysis solution is an important part of robotic technology of the mining automatic extraction manipulators FEM-5 and FEM-6 because manipulating can be executed through moving the cutting crown and connected with it parts in three-dimensional Euclidean space. Such operations include positioning (advancing) and orientation (common rotation) of the FEM-5 operating member.

It is known that cutter crown of FEM-5 consists of rigid segments which allows using the apparatus for the solid body description. In reality all manipulation robots are built of flexible elements. Nevertheless, approaches of such kind are not included into operation due to their complexity.

According to Fig. 3, let us imagine the cutter crown as a sequence of rigid segments connected with each other by sequence N of prismatic or revolute joints. Independent and free move of each joint may be considered as degree of freedom associated with the independent forced motion of displacement field q_m, m =1,2...N, FEM-5. On the other hand, change of the FEM-5 end segment orientation can be described by means of changes in six-dimensional coordinate system $x_i = [\rho_x \rho_y \rho_z \theta \varphi \psi]$, of coordinate system of the end segment T_0^n, so that $p = [\rho_x \rho_y \rho_z]^T$ – vector of position for the beginning of coordinate system T_0^n, and 0, θ, φ и ψ – Eulerian angles or angles of rotation, inclination, horizontal and vertical swings of transformation T_0^n linking п- system of coordinates with the basic coordinate system x_0, y_0, z_0.

Kinematic research objectives concerning the executive boom-like mechanisms of the mining automatic extraction manipulator and techniques of their solution have their own peculiarities. In robotic mechanics direct and inverse tasks of kinematics are solved, kinematic synthesis from the condition of the assigned service area formation is executed. The executive boom-like mechanisms of the mining automatic extraction manipulator being the subject of this work research contain the closed kinematic circuits as a part of RTC of FEM-5 mining automatic manipulator.

7 Conclusion

Kinematic and dynamic models of the manipulators were built and researched. At that mathematic model of calculating the cutting forces and feeding on the operating member cutters as well as loads on the mining automatic extraction manipulator of flanking-frontal-selective action depending on the kinematic parameters of possible modes of the coal face treatment are developed. Trajectories of the manipulator's operating member tip advancing, movement of the front plane and in the plane of i-cutter obtained by means of simulation modeling in MatLab at the assigned parameters are determined. Besides, parameters of the mining automated extraction manipulator with account of accuracy of the cutting seams determination are stated.

It is shown that at the mode of the crown penetration into the broken massif the feeding speed increase in greater degree than energy consumption increases the loads; and these instantaneous values linearly depend on the time of manipulator operation. At the mode of coal drawing throughout entire thickness of seam without manipulator delivery the loads and specific energy consumption are constant; at that the loads of the manipulator swinging speeds increase whereas the specific energy consumption decreases. At combining the manipulator swinging speed with the speed of delivery along the face the loads and specific energy consumption are directly proportional and depend on the operation time and increase with the increase of speed.

Analysis and synthesis of system for the electric hydraulic valves control by the manipulator drives were conducted and, exactly, the FEM-5 load regulator and systems of self-regulation were selected. They were selected to reduce dispersion and to increase mathematical expectation up to the nominal value which gives the possibility of using microprocessor system for control of the robotic technology complex.

Results of the check in MatLab environment for stability according to Hurwitz criterion, simulation modeling of the FEM-5 manipulator's working part i-cutter movement are obtained. Diagrams of the closed-loop system transient time, transfer function of the closed-loop subsystem for control in vertical and horizontal planes are obtained as well as Bode Plot, Nyquist, Root Locus diagrams' characteristics were examined.

Data of transfer function were considered as for two-stage segment the tracking drive feeding spool is the input parameter while the fluid consumption is the output parameter. Accuracy of reproducing with account of the error values is provided. Logarithmic amplitude characteristics (LAC) is obtained for determining the coordinates of control point aimed at prohibited area building at the correcting segment operation which provides the accuracy of the executive mechanisms motion at mining the face by FEM-5. Computer modeling and numerical experiments were implemented in MatLab software.

Acknowledgement

The research group acknowledges all contributors to the study of Development of Coal Mining Robotic Automation Project which has been implemented in the enterprises of Karaganda Coal Mine (Kazakhstan) and Karaganda State Polytechnic University. Also, the research group wants to thank all scientists and support team who were dealing with development and designing of mining automation process both in academia and industry.

References

[1] *Concept of Development of Coal Mining in Republic of Kazakhstan till 2020: verified by Government of Kazakhstan's Act #644 in 28th June 2008, Astana, p. 23 (in Russian)*
[2] *LI Yunwang, GE Shirong, ZHU Hua, FANG Haifang, GAO Jinke Mobile platform of roker-type coal mine rescue robot. Mining Science and Technology 2010; 20: 0466-0471*
[3] *Muratbek Arpabekov Adaptive-programming controil of robotic complex. Saint-Petersburg State University's Sientific-Technical Vedomosts, Saint-Petersburg, 2010, №2 (97): 63-70 (in Russian)*
[4] *M.Shakhinpur Basics of Robotics. translated to Russian by S.Dmitrieyv, Mir 1990, Moscow, p. 527 (in Russian)*
[5] *Jonathon C. Ralston, Andrew D. Strange Developing selective mining capability for longwall shearers using thermal infrared-based seam tracking. International Journal of Mining Science and Technology 2013; 23: 47-53*
[6] *Ralston Jonathon, Reid David, Hargrave Chad, Hainsworth David Sensing for advancing mining automation capability: A review of underground automation technology development. International Journal of Mining Science and Technology 2014; 24: 305-310*
[7] *T. Ermekov, K. Sholanov, M.Arpabekov Sientific fundandamental solving and choosing parameters of mining and construction robotic complex, Evero 2009, Almaty, p. 272 (in Russian)*
[8] *Muratbek Arpabekov. Modelling of FEM-5 working process in analog comptuting systems. Proceedings of Conference "The development of the theory and practice of fundamental and applied sciences", Federal Agency for Education and Penza State University of Architecture and Construction (PGUAS) 2009, Penza (Russia), p. 138-142 (in Russian)*
[9] *N. Bruslenko Modelling complex systems, Moscow 1978, p.399 (in Russian)*
[10] *Muratbek Arpabekov Mathematical model of mining shearer and its cutting drum position. Proceedings of International Conference "Actual problems of mathematics, computer science, mechanics and control theory "dedicated to the 60th anniversary of professor, academician R. Biyarova, Institute of Mechanics and Mechanical Engineering of MES RK (in Russian)*
[11] *Toleukhan Ermekov, Muratbek Arpabekov Geometric shapes of mining shearer' working parts and its possible ways of control, Proceedings of International Conference dedicated to 45th Anniversarry of TzECI "Modern architecture, construction and transport: current status and prospects and development", L.N. Gumiloyv ENU 2009, Astana, p. 99-102 (in Russian)*
[12] *Toleukhan Ermekov, Muratbek Arpabekov Mining Machine. By recommendation of Ministry of Education and Science of Republic of Kazakhstan for professional educational institutions, Foliant 2009, p. 372 (in Russian)*